Original Research Article (Experimental)

# The combination of *Elephantopus scaber* and *Phaleria macrocarpa* leaves extract promotes anticancer activity via downregulation of ER-α, Nrf2 and PI3K/AKT/mTOR pathway

Yuyun Ika Christina [a], Muhaimin Rifa'i [b], Nashi Widodo [b], Muhammad Sasmito Djati [b, *]

[a] *Doctoral Program, Department of Biology, Faculty of Mathematics and Natural Sciences, Brawijaya University, Malang 65145, East Java, Indonesia*
[b] *Department of Biology, Faculty of Mathematics and Natural Sciences, Brawijaya University, Malang 65145, East Java, Indonesia*

## ARTICLE INFO

## ABSTRACT

*Background:* *Elephantopus scaber* and *Phaleria macrocarpa* have recently been interested as novel anticancer agents. However, there was no scientific evaluation of the anticancer effect of both plant combinations.
*Objective:* This study investigated the potential anticancer effects of combined *E. scaber* and *P. macrocarpa* leaves extract on human breast cancer cells lines.
*Materials and methods:* T47D cells were treated with the combination of *E. scaber* and each part of *P. macrocarpa* (leaves/EL, mesocarp/EM, seed/ES and pericarp/EP). T47D cells were then exposed to three ratios (1:1, 2:1, and 1:2) of the best combination for 24, 48, and 72 h. The cell viability of T47D and TIG-1 cells was assessed using WST-1 assay. The apoptotic hallmarks were determined using FITC Annexin V-PI staining and DNA fragmentation assay. The cell proliferation and cell cycle profiles were analyzed using CFSE (carboxyfluorescein succinimidyl ester) and Propidium iodide-flowcytometry assays. The relative number of p-ERα, p-Nrf2, p-PI3K, p-AKT, and p-mTOR were assessed using flow cytometry. The molecular docking analysis was also performed to confirm the mechanism of the extract in silico.
*Results:* The combination of *E. scaber* and *P. macrocarpa* leaves (EL) possessed strong cytotoxic activity (p < 0.05) than other combination groups and cisplatin. EL showed selective killing only to T47D cells. EL at a ratio of 2:1 potentially suppressed the cell viability and cell division, induced apoptosis, and arrested the cell cycle of T47D cells by triple inhibiting the p-Nrf2, p-ERα, and p-PI3K/AKT/mTOR signaling pathway. Molecular docking analysis confirmed that the possible mechanism of EL to reduce T47D cell growth was by inhibiting ERα and Nrf2-complex, resulting in the reduction in the crosstalk effect of Nrf2, ERα and PI3K/AKT/mTOR pathways.
*Conclusion:* The combination of leaf extracts from *E. scaber* and *P. macrocarpa* caused cell death in breast cancer cells T47D and not in normal cells TIG-1; hence has the potential to show anticancer efficacy in preclinical and clinical trials.

## 1. Introduction

Breast cancer is the most common cancer diagnosed in women worldwide [1]. In 2020, Global Cancer Observatory estimated that female breast cancer cases about 2.3 million (11.7% of all cancer types) [2]. Various therapies, such as chemotherapy and radiotherapy, were used to eliminate breast cancer cells. Unfortunately, the chemotherapy drug had a cytotoxicity effect on cancer and healthy cells [1,3]. Radiotherapy is also used to treat cancer, but this treatment has a radio-resistant impact that leads to treatment failure [4]. The use of natural plant products for clinical development has developed tremendously in recent decades [5]. Medicinal plants and their bioactive compounds are identified as potent treatments for cancer due to their selective effect, demonstrating a non-toxic impact on normal cells and a cytotoxic effect on cancer cells [6]. In Indonesia, various experimental studies have indicated anticancer activities from various herbal medicines such as Mahkota Dewa (*Phaleria macrocarpa* (Scheff.) Boerl) and Tapak Liman (*Elephantopus scaber* Linn.).

*E. scaber* Linn. belongs to the Asteraceae family and is a genus of perennial herb widely spread in Asia, Tropical Africa, India and Australia [7]. In Indonesia, the plant is commonly known as Tapak Liman and is used for traditional medicine. *E. scaber* can be used as an antidiuretic, antiviral, antibacterial agent and is traditionally used to treat hepatitis, cough, pneumonia and bronchitis [8−10]. Sesquiterpenes lactones are abundant in all *E. scaber* parts, including deoxyelephantopin, isodeoxyelephantopin, scabertopin, and isoscabertopin, which is a potent anticancer compound [11]. Lupeol isolated from *E. scaber* also induce apoptosis in MCF-7 cell by downregulating Bcl-2 and Bcl-xL protein [12].

*P. macrocarpa* (Scheff.) Boerl is mainly known as East Asian herbal medicine, which is traditionally used to remedy various diseases, including diabetes mellitus, liver and heart disease, cancer, kidney disorder, skin, and stroke [13]. Many pharmacological effects have been studied over the year, including anticancer, antioxidant, antidiabetic, anti-inflammatory, and antibacterial activity [14]. The methanol extract of *P. macrocarpa* seed possessed a cytotoxic effect against HT-29, MCF-6 Cas Ki, and SKOV-3 cell lines and produced mild toxicity in MRC-5 cells [15]. Christina et al. [16] revealed that *P. macrocarpa* leaves could inhibit the growth of T47D cell lines with $IC_{50}$ value of 97 μg/mL.

ERα is mainly contributed to the initiation and progression of breast cancer with ER-positive. The activation of ERα causes phosphorylation of IGF-1R, EGFR and IRS1 and then leads to activation of PI3K downstream, such as AKT1 and mTOR. ER-α also directly activated p85 as a regulatory subunit of PI3K protein. Then, the downstream protein is still activated and leads to the progression of tumor growth and survival [17]. In this study, we used T47D cells with ER-positive and upregulation of Nrf2. Nrf2 is one of the targets downstream of PI3K and ERα. Upregulation of Nrf2 could promote the survival of breast cancer [18]. Therefore, there is a crosstalk between ERα, Nrf2 and PI3K/AKT/mTOR, which upregulation of those pathways leads to an increase in breast cancer growth and survival. Targeting those pathways is a promising strategy to inhibit the growth and survival of breast cancer cells.

The use of plant extract combinations can be developed as a potent therapy for breast cancer. Otieno et al. [19] and Christina et al. [8] revealed that the mixture of several plant extracts had larger bioactivity than a single plant extract as an antibacterial agent. However, to the best of our knowledge, there is no scientific evaluation on using the multi-plant extract for treating breast cancer, especially *P. macrocarpa* and *E. scaber*. Considering the crucial need to develop novel therapeutic strategies for breast cancer, the present study aimed to investigate the potential anticancer effects of combined *E. scaber* and each plant part of *P. macrocarpa* extract and its underlying mechanism to inhibit T47D cell growth. We also used TIG-1 cells to determine the selectivity and safety of the plant extract on normal cells. This study is the first experiment revealing the anticancer activity of the combination plant extract.

## 2. Materials and methods

### 2.1. Plant materials and extraction

The fresh leaves and fruit of *P. macrocarpa* and leaves of *E. scaber* were collected from UPT. Laboratorium Herbal Materia Medica Batu, Indonesia. A voucher specimen for *E. scaber* (074/228/102.7/ 2018) and *P. macrocarpa* (No. 074/384A/102.7/2020) was deposited at the herbarium of the UPT. Laboratorium Herbal Materia Medica Batu, Indonesia. The seed, mesocarp and pericarp of *P. macrocarpa* fruit were separated. All samples were washed with tap water, dried, and blended. Briefly, the powdered sample of all plant samples was subjected to ethanol extraction, as Christina et al. [8] and Djati et al. [20] described. A total of 200 g of each powdered sample was extracted with 2 L of 95% ethanol for $3 \times 14$ h at room temperature in a dark place. Each sample was filtered and then evaporated at 50 °C using a rotary evaporator (IKA® RV 10, IKA Works (Asia) Sdn Bhd, Malaysia). All extracts were stored at 4 °C for further analysis.

A total of 10 mg dry weight of ethanol extract of each sample was dissolved in 5 mL RPMI-1640 for T47D treatment and 5 mL MEM for TIG-1 cells. After mixing, each diluted sample was then filtered using 0.22 μm syringe filter (Minisart®, Sartorius AG, Germany). The concentration of extract stock was 10 mg/mL medium and then prepared for treatment medium based on $IC_{50}$ value of each extract. The $IC_{50}$ values of leaves, mesocarp, seed and pericarp of *P. macrocarpa* on T47D were 97, 144, 139, and 125 μg/mL, respectively, obtained from our previous study [16]. While the $IC_{50}$ value of *E. scaber* against T47D was 121 μg/mL, obtained from our previous study (in review).

### 2.2. Cell cultures

The human breast cancer cell line, T47D (ATCC®) was purchased from Cancer Chemoprevention Research Center (CCRC), Faculty of Pharmacy, Universitas Gadjah Mada, Indonesia. The normal human fibroblast cell line, TIG-1, was obtained from JCRB Cell Bank (Japanese Collection of Research Bioresources Cell Bank), National Institutes of Biomedical Innovation, Health and Nutrition, Japan. T47D and TIG cell lines were used between passages number 20−25. T47D cells were cultured in Roswell Park Memorial Institute 1640 medium (RPMI), supplemented with 10% fetal bovine serum (FBS) and 1% antibiotic (100 U/mL penicillin and 100 μg/mL streptomycin). TIG-1 cell lines were maintained in Minimum Essential Media (MEM) supplemented with 10% fetal bovine serum (FBS) and 1% antibiotic (100 U/mL penicillin and 100 μg/mL streptomycin). These cell lines were incubated at 37 °C in humidified air with 5% $CO_2$ incubator.

### 2.3. Apoptosis investigation

T47D cells ($5 \times 10^4$ cells/ml) were seeded in 24-well plates and incubated for 24 h at 37 °C in humidified air with 5% $CO_2$ incubator. Cells were treated with the combination of $IC_{50}$ value of *E. scaber* and each $IC_{50}$ value of leaves (EL), mesocarp (EM), seed (ES) and pericarp (EP) of *P. macrocarpa* in ratio 1:1. The best combination ratio was found in EL group. Then, cells were treated with three ratios of the best combinations (2:1, 1:1, and 1:2) for 24, 48, and 72 h. The composition of ratio 2:1, 1:1 and 2:1 was $2 \times IC_{50}$ value (242 μg/mL) of *E. scaber* leaves and $1 \times IC_{50}$ value (97 μg/mL) of *P. macrocarpa* leaves, $1 \times IC_{50}$ value (121 μg/mL) of *E. scaber* leaves and $1 \times IC_{50}$ value (97 μg/mL) of *P. macrocarpa* leaves, and $1 \times IC_{50}$ value (121 μg/mL) of *E. scaber* leaves and $1 \times IC_{50}$ value (194 μg/mL) of *P. macrocarpa* leaves, respectively.

Cells were subsequently harvested for 24, 48 and 72 h by using trypsinization and centrifuged at 2500 rpm for 5 min. Then, 100 μl of cell suspension was transferred to a 1.5 mL microtube. Each sample was added with 2 μl of Annexin V-FITC, 4 μl of Propodium iodide (PI) and 44 μl of binding buffer and then gently mixed and incubated for 20 min. Data were collected (10,000 events/sample) using a Flow cytometer (BD FACS Calibur™, San Jose, CA). FACS data were analyzed using FlowJo™ v. 10 Software (Vancouver, BC). The cell population in different quadrants were analyzed. The lower right (LR) indicated early apoptotic cells, the upper right (UR) indicated late apoptotic cells, the upper left (UL) indicated necrotic cells, and the lower left (LL) indicated live cells.

## 2.4. Cell viability assay and cell imaging

Briefly, T47D cells ($5 \times 10^3$ cells) were seeded in each well of a 96-well plate for 24 h. Cells were treated with three ratios of the best combination extract (1:1, 1:2, and 2:1) for 24, 48 and 72 h at 37 °C, 5% $CO_2$. Then, the medium was removed and replaced with a complete medium containing 5 µl/well of 4-[3-(4-Iodophenyl)-2-(4-nitro-phenyl)-2H-5-tetrazolio]-1,3-benzene sulfonate (WST-1) reagent (Sigma-Aldrich, Inc., USA) for 30 min. The plate was shaken thoroughly for 1 min. The absorbance of the sample was measured using a microplate (ELISA) reader (BioTek Instruments, Inc., USA) against blank at 450 nm. All experiment was carried out in triplicate. The cell viability was determined with the following formula:

$$Cell\ viability\ (\%) = \frac{A_{sample} - A_{blanko}}{A_{control} - A_{blanko}} \times 100$$

T47D cells were observed and captured using Olympus Inverted Microscopes Models IX71 (NY, USA) with 200× magnification for cell morphology analysis.

## 2.5. DNA fragmentation assay

T47D cells were treated with three ratios of the best combination extract (1:1, 2:1, and 1:2) for 72 h. The DNA of harvested cells was then extracted using DNA purification kit, which is the procedure according to the manufacturer's protocol of NEXPrep™ Cell/Tissue DNA Mini Kit (NEX Diagnostics, Korea). The obtained DNA from each group was analyzed using electrophoresis on 1.5% agarose, 100 V, 60 min. The gel was stained with Diamond™ Nucleic Acid Dye (Promega Corporation™, USA) and captured in a CCD imager (ImageQuant™ LAS 500, USA) with 1 kb DNA ladder (Promega Corporation™, USA) as a marker.

## 2.6. CFSE proliferation assay

T47D cells ($5 \times 10^4$ cells/mL) were seeded in 24 well plates and incubated at 37 °C in humidified air with 5% $CO_2$ incubator. After 24 h, T47D cells were harvested and washed with 500 µL Phosphate Buffer Saline (PBS). Cells were stained with 5 µM of CFSE (carboxyfluorescein succinimidyl ester) (ThermoFisher™ Scientific), incubated for 20 min at 37 °C and added 500 µL PBS. Cells were then washed with 500 µL PBS once and PBS twice. Stained cells were then seeded in 24 plates with a density of $3 \times 10^5$ cells, followed by incubation for 24 h. Then, cells were treated with EL, EM, ES and EP in ratio 1:1 and three different ratios of the best combination (1:1, 2:1, and 1:2) for 24, 48, and 72 h. The CFSE fluorescence intensity was determined by flow cytometry using a flow cytometer (BD FACSCalibur™, San Jose, CA, USA) and analyzed using FlowJo™ v. 10 Software (Vancouver, BC).

## 2.7. Cell cycle phase distribution

Briefly, cells were treated with EL, EM, ES, and EP in ratio 1:1 and three different ratios of the best combination (1:1, 2:1, and 1:2) for 24, 48, and 72 h. Then, cells were harvested and centrifuged at 2500 rpm for 5 min. The pellet was washed with 1 mL PBS and centrifuged at 2500 rpm for 5 min. Cells were then suspended with 500 uL of 70% ethanol for 30 min. Then, cells were washed with 500 uL PBS twice by centrifugation at 2500 rpm for 5 min. Cells were stained with 5 µL of Propidium Iodide (500 µg/mL). After 30 min incubation, data were collected (10,000 events/sample) using a Flow cytometer (BD FACS Calibur™, San Jose, CA, USA) and analyzed using FlowJo™ v. 10 Software (Vancouver, BC).

## 2.8. The relative number of p-Erα, p-Nrf2, p-PI3K, p-AKT and p-mTOR

Briefly, T47D cells were treated with EL, EM, ES, and EP in ratio 1:1 and three different ratios of the best combination (1:1, 2:1, and 1:2) for 24 and 48 h. Harvested cells were centrifuged at 2500 rpm for 5 min. Then, 100 µL of cell suspension was added with 50 µL of Intracellular (IC) fixation buffer (eBioscience™, Invitrogen, Thermo Fisher Scientific, USA) and incubated for 20 min in a cool box. After incubation, each sample was added with 500 µL of diluted Permeabilization Buffer (Invitrogen, Thermo Fisher Scientific, USA) and centrifuged at 2500 rpm for 5 min.

Pellets were then stained with the following antibody: PE-Phospho-PI3K p85/p55 (Tyr458, Tyr199) Recombinant Rabbit Monoclonal Antibody (Catalog no. MA5-36954), PE-Phospho-AKT1 (Ser473) Monoclonal Antibody (Catalog no. 12-9715-42), PE-Phospho-mTOR (Ser2448) Monoclonal Antibody (Catalog no. 12-9718-4), Phospho-Estrogen Receptor alpha (Tyr537) Monoclonal Antibody (Catalog no. MA5-31845) with conjugate of FITC-Goat anti-Mouse IgG (H + L) Cross-Adsorbed Secondary Antibody (Catalog no. F-2761), and Phospho-Nrf2 (Ser40) Recombinant Rabbit Monoclonal Antibody (Catalog no. MA5-32116) with the conjugate of FITC-Goat anti-Rabbit IgG (H + L) Cross-Adsorbed Secondary Antibody (Catalog no. F-2765). All antibodies were purchased from Invitrogen, Thermo Fisher Scientific, USA. The relative number of p-PI3K, p-AKT1, p-mTOR, p-Nrf2, and p-ERα were measured using a flow cytometer (BD FACS Calibur™, San Jose, CA) and analyzed with FlowJo™ v. 10 Software (Vancouver, BC).

## 2.9. Molecular Docking analysis

The three selected bioactive compounds (apigenin, coumaric acid and sesamin) of *P. macrocarpa* leaves were obtained from Liquid Chromatography-High Resolution Mass Spectrometry (LC-HRMS) analysis based on our previous study [21]. While the three selected compounds from *E. scaber* extract (oleanolic acid, scabertopin, scutellarin) were obtained from our previous study (in review). The compounds were retrieved in.sdf format from PubChem database (https://pubchem.ncbi.nlm.nih.gov/) and converted into.pdb format using PyMol (Schrödinger Inc., LLC). Each ligand was then minimized using Open babel in Pyrx 0.8 (The Scripps Research Institute, California). The 3D structure of protein target Erα ($1 \times 7R$) and Nrf2-Keap1 complex (4IQK) were obtained from Protein Data Bank (PDB) (https://www.rcsb.org/). The water molecules and unnecessary ligands of protein were removed. Tamoxifen (Pubchem ID: 2733526) and AEM-1 (Pubchem ID: 9196193) were used as a natural inhibitors for ERα and Nrf2, respectively. Ligands docking to ERα was set to x = 10.2328, y = 27.3348, z = 8.4267 with dimensions (angstrom) x = 13.5222, y = 12.6181, z = 16.1499, and Nrf-2 was set to x = −32.8510, y = −0.8653, z = −17.2136 with dimensions (angstrom) x = 15.1608, y = 10.0973, z = 10.0340. Molecular docking was performed using Pyrx 0.8, then visualized in PyMol and evaluated its amino acid interaction using Biovia Discovery Studio v20 (Dassault System, Biovia corp.) [22].

## 2.10. Statistical analysis

All data were expressed as mean ± SD for three independent experiments. Statistical analysis using two-way ANOVA followed the Tukey test, which SPSS performed for Windows version 22. The data were considered significantly different if the p-value <0.05. All graphs/bars were visualized using GraphPad Prism 8 (GraphPad Software, San Diego, CA, USA).

# 3. Results

## 3.1. EL induced apoptosis on T47D cells

T47D cells significantly ($p < 0.05$) entered early and late apoptosis stages after being treated with all combination extract and cisplatin (Fig. 1A). EL group possessed the higher time-

dependent increase in late and early apoptotic cells (Fig. 1B) followed by a high reduction in live cells compared to cisplatin. Interestingly, the lowest percentage of necrotic cells was found in the EL group. Compared to untreated cells, EL at the ratio of 2:1 significantly ($p < 0.05$) reduced the live cells population in a time-dependent manner (Fig. 2A). Furthermore, the ratio of 2:1 significantly induced a higher percentage of late apoptotic cells in a time-
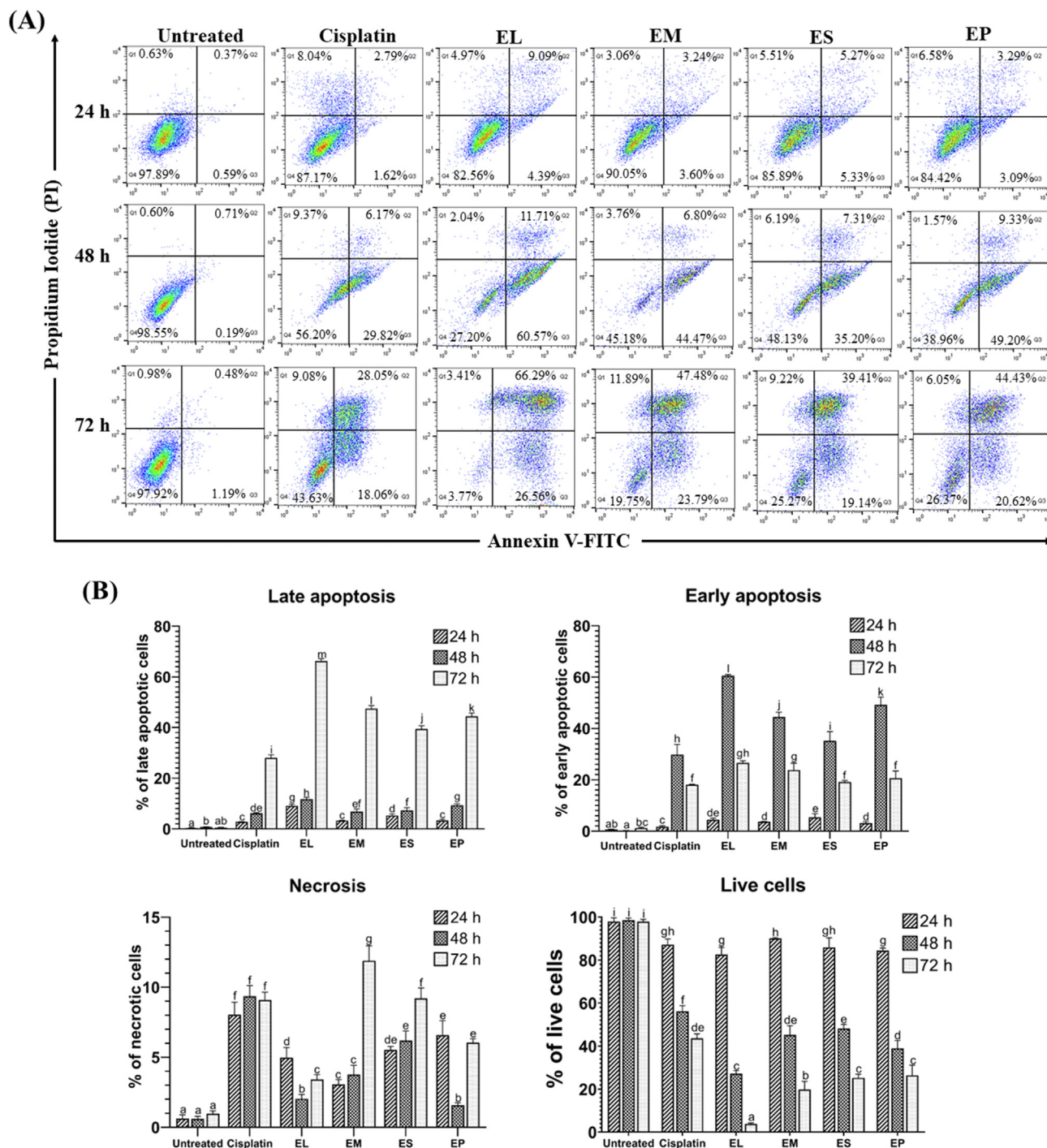


**Fig. 1.** Flow cytometry analysis of apoptosis in T47D cells after being treated with the combination of *E. scaber* and each plant part of *P. macrocarpa* extract using FITC Annexin V/PI staining. Untreated cells and cisplatin were used as negative and positive controls, respectively. (A) The representative dot plots indicate that T47D cells undergo necrosis (Q1/upper left quadrant), late apoptosis (Q2/upper right quadrant), early apoptosis (Q3/low right quadrant) and live cells (Q4/low left quadrant) after 24, 48, and 72 h treatment with (A) EL, EM, ES and EP in ratio 1:1. (B) The graph showed the quantification of apoptosis levels in all experiment groups. The mean values ± standard deviation (SD) were expressed from three independent experiments. The different letters indicated statistical differences ($p < 0.05$). EL: *E. scaber + P. macrocarpa* leaves; EM: *E. scaber + P. macrocarpa* mesocarp; ES: *E. scaber + P. macrocarpa* seed; EP: *E. scaber + P. macrocarpa* pericarp.
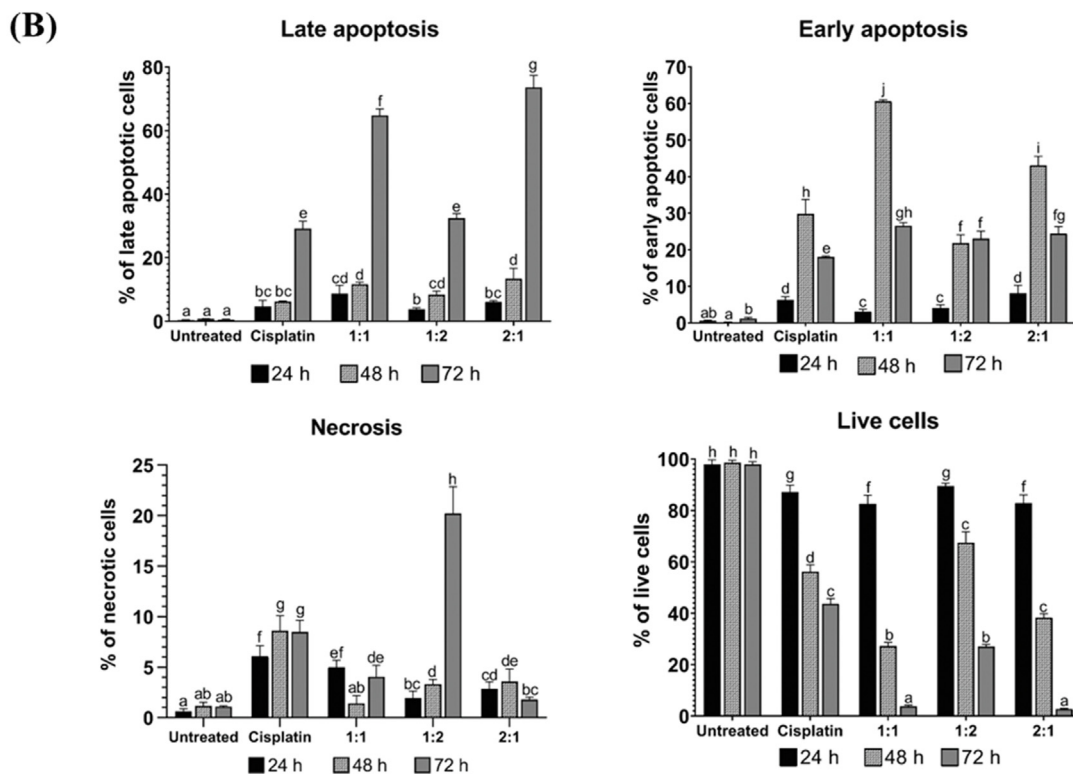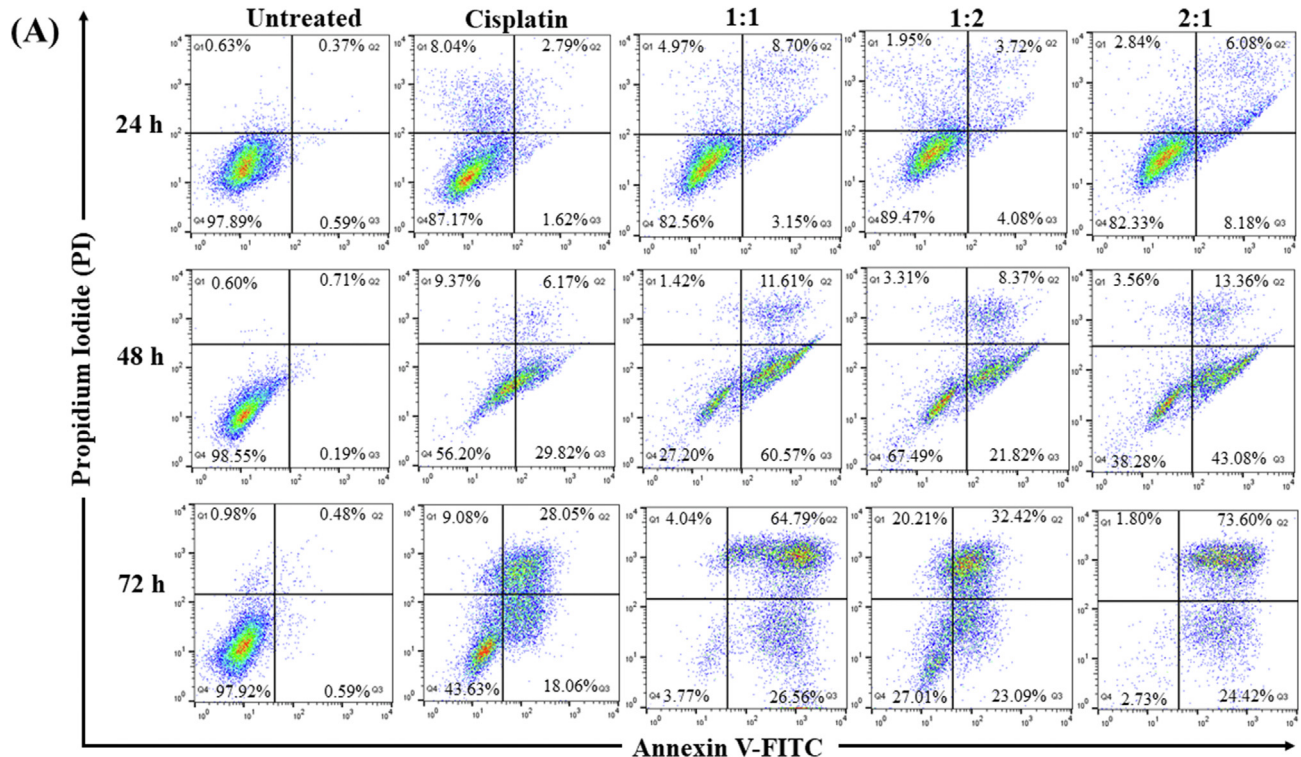
**Fig. 2.** Apoptosis detection by flow cytometry based on FITC-Annexin V/PI labelling in T47D cells. T47D cells were treated with combined *E. scaber* leaves and *P. macrocarpa* leaves extract (EL) at three different ratio combinations (1:1, 1:2, and 2:1) for 24, 48, and 72 h. Untreated cells and cisplatin were used as negative and positive controls, respectively. (A) Representative dot plots indicated that apoptosis cells could be detected by increased fluorescence intensity of double-positive Annexin V/PI. The necrotic cell (Q1/upper left quadrant), late apoptotic cells (Q2/upper right quadrant), live cells (Q3/lower left quadrant) and early apoptotic cells (Q4/lower right quadrant). (B) Percentage of necrotic, live, early and late apoptotic cells in all experiment groups. The mean values ± standard deviation (SD) were expressed from three independent experiments. The different letters indicated statistical differences (p < 0.05). 2:1 = 2 × $IC_{50}$ value of *E. scaber* leaves and 1 × $IC_{50}$ value of *P. macrocarpa* leaves; 1:2 = 1 × $IC_{50}$ value of *E. scaber* leaves and 2 × $IC_{50}$ value of *P. macrocarpa* leaves.

dependent manner (p < 0.05) compared to cisplatin. The numbers of early apoptotic cells were increased at a ratio of 1:1, followed by a ratio of 2:1 after 48 h incubation (Fig. 2B). Interestingly, a low number of necrotic cells was found in the ratio of 2:1. These results indicated that EL effectively induced the highest apoptotic cells, followed by low necrotic cells (see Fig. 2).

### 3.2. EL reduced cell viability and induced DNA fragmentation, followed by morphological changes in T47D cells

The results revealed that untreated T47D cells displayed normal morphology and did not degrade their DNA into nucleosomal size fragments indicated by a single DNA band (Fig. 3A). When treated with all ratios of EL and cisplatin, T47D cells exhibited DNA fragments as shown by typical DNA laddering compared to marker. The appearance of DNA fragments in all treatment groups ranged from 500 to 10,000 bp.

After 24 h of treatment, the highest reduction in cells viability was observed in the cisplatin group, followed by the EL group at 1:1 and 2:1 (34.63% versus 44.31% 44.64%) (Fig. 3B). The high decrease in the viability of T47D cells was found in the ratio of 2:1 (10.17%) at 48 h, followed by cell morphological changes. All combination groups caused the changes in cell shape into rounding and floating cells, the appearance of nucleus condensation (yellow arrow), blebbing in the cell membrane (red arrow), and then the formation of apoptotic bodies (green arrow). These characteristics were more observed in the combination group than in the cisplatin group (Fig. 3D). These results align with the apoptosis assay results that the cisplatin group exhibited a high percentage of necrotic cells (black arrow) compared to the combination group.

Interestingly, the normal fibroblast cell line (TIG-1) responds differently to the EL combination. TIG-1 cells showed 85−93% of viability after 24 h of treatment in all ratios of EL, but the cisplatin group exhibited only 65.34% of viability simultaneously (Fig. 3C). Ratio of 2:1 was not significantly (p > 0.05) different from the ratio of 1:2. These findings align with the morphological assessment of TIG-1 cells, as displayed in Fig. 3E. An elongated fibroblast-like cell morphology less rounded and floating cells were observed in all ratios of EL. However, the cisplatin group exerted more rounded and floating cells. Therefore, the EL combination appears to have a selective effect against breast cancer but less affects the viability of normal fibroblast TIG-1 cells.

### 3.3. EL abrogates the proliferation of T47D cells

The untreated cells demonstrated a reduction in CFSE staining, which indicated cell proliferation in T47D cells (Fig. 4A). The percentage of proliferating T47D cells was significantly decreased after being exposed to all combinations and cisplatin groups. EL group exhibited a high reduction (p < 0.05) in the percentage of proliferating cells at 24 h of treatment compared to the cisplatin, EM, EB, and EP group (Fig. 4C). At 48 and 72 h, the EL group also abrogates the proliferating cells at a high number and is similar to the cisplatin group. EM group could only reduce proliferating cells at a high number after 72 h. These data indicate that EL could reduce the higher proliferating cells in T47D cells compared to other combinations. Ratios 1:1 and 2:1 exhibited a high decrease in proliferating cells, which are not significantly different from the cisplatin group (Fig. 4B and D).

### 3.4. EL arrested the cell cycle of T47D cells

As shown in Fig. 5A, the cisplatin group exhibited a high accumulation of apoptotic cells (sub-G1 phase) followed by a reduction

in the G2/M phase was clearly observed after 72 h. Compared to other combinations, the EL group effectively (p < 0.05) increased the apoptotic cells in a time-dependent manner (Fig. 5B). These data were in line with the apoptotic results, in which EL have a higher percentage of late and early apoptotic cells. EL group also exhibited an increased accumulation in G0/G1 phase at 24 h, followed by a high reduction in the S phase at 24 h and G2/M phase at 72 h.

The results demonstrated that the different ratio of EL significantly affects the cell cycle distribution of T47D cells (Fig. 5C). The number of proliferating cells (G2/M) was markedly decreased (p < 0.05) in T47D cells after being exposed to EL at the ratio of 2:1 (Fig. 5D). EL also induced high apoptotic cells time-dependent, followed by accumulation of G0/G1 and reduction in the S phase at 24 h. These data confirmed that the ratio of 2:1 could inhibit the growth of T47D cells not only by G2/M arrest but also by triggering apoptosis due to a high increase of the sub-G1 phase.

### 3.5. EL inhibited phosphorylated-Nrf2 and ER-α in T47D cells

The untreated cells exhibited a high number of phosphorylated Erα and Nrf2. After 48 h of incubation, the lowest expression of p-ERα was observed in a ratio of 1:1 (Fig. 6A). Furthermore, the exposure of all ratios of EL to T47D cells resulted in the down-regulation of p-Nrf2 after 24 h (Fig. 6B). Cisplatin group exhibited the highest reduction of Nrf2 at 24 h. After 48 h, the highest inhibition of p-Nrf2 was observed in the ratio of 1:1, but not significantly different from a ratio of 1:2. These results suggested that the EL reduced the cell proliferation of T47D cells by suppressing p-Nrf2 and p-ERα.

### 3.6. EL suppressed the phosphorylated-PI3K, AKT and mTOR in T47D cells

Compared to untreated cells, the ratio of 1:1 showed a high decrease in p-PI3K expression, followed by a ratio of 2:1 (Fig. 6C). However, all extract combinations were not significantly different after 48 h of treatment. Interestingly, the deficient level of p-AKT was observed in a ratio of 2:1 in a time-dependent manner, followed by ratios 1:1 and 1:2 (Fig. 6D). While the expression of p-mTOR dramatically declined after treatment with EL with the ratio of 1:1 for 24 h (Fig. 6E). The level in p-PI3K, p-AKT and p-mTOR in the combination group was lower than cisplatin. Therefore, EL at ratio of 2:1 mostly has an anti-proliferative activity by downregulating the phosphorylation of PI3K/AKT/mTOR cascades.

### 3.7. Molecular docking analysis

Three identified compounds of *E. scaber* (oleanolic acid, scabertopin, and scutellarin) and *P. macrocarpa* leaves (apigenin, sesamin, and coumaric acid) were evaluated for their interaction with ERα and Nrf2. We used molecular docking to determine the mechanism insight of those bioactive compounds to modulate ERα and Nrf2 expression. The results demonstrated that the three-dimensional structure of tamoxifen (Fig. 7) showed interaction to ERα with eight van der Waals forces on Gly390, Leu320, Leu387, Leu403, Lys449, Phe445, Pro324, and Val446 (Table 1). Interestingly, scutellarin from *E. scaber* and sesamin from *P. macrocarpa* leaves strongly interacted with ERα and gave a stronger binding affinity (−7.6 kcal/mol and −8.5 kcal/mol, respectively) than tamoxifen as a control drug (−6.7 kcal/mol). Scutellarin interacted with ERα through four hydrogen bonds on Arg394, Ile386, Pro325 and Trp393 and eight van der Waals forces on Glu353, Glu397,
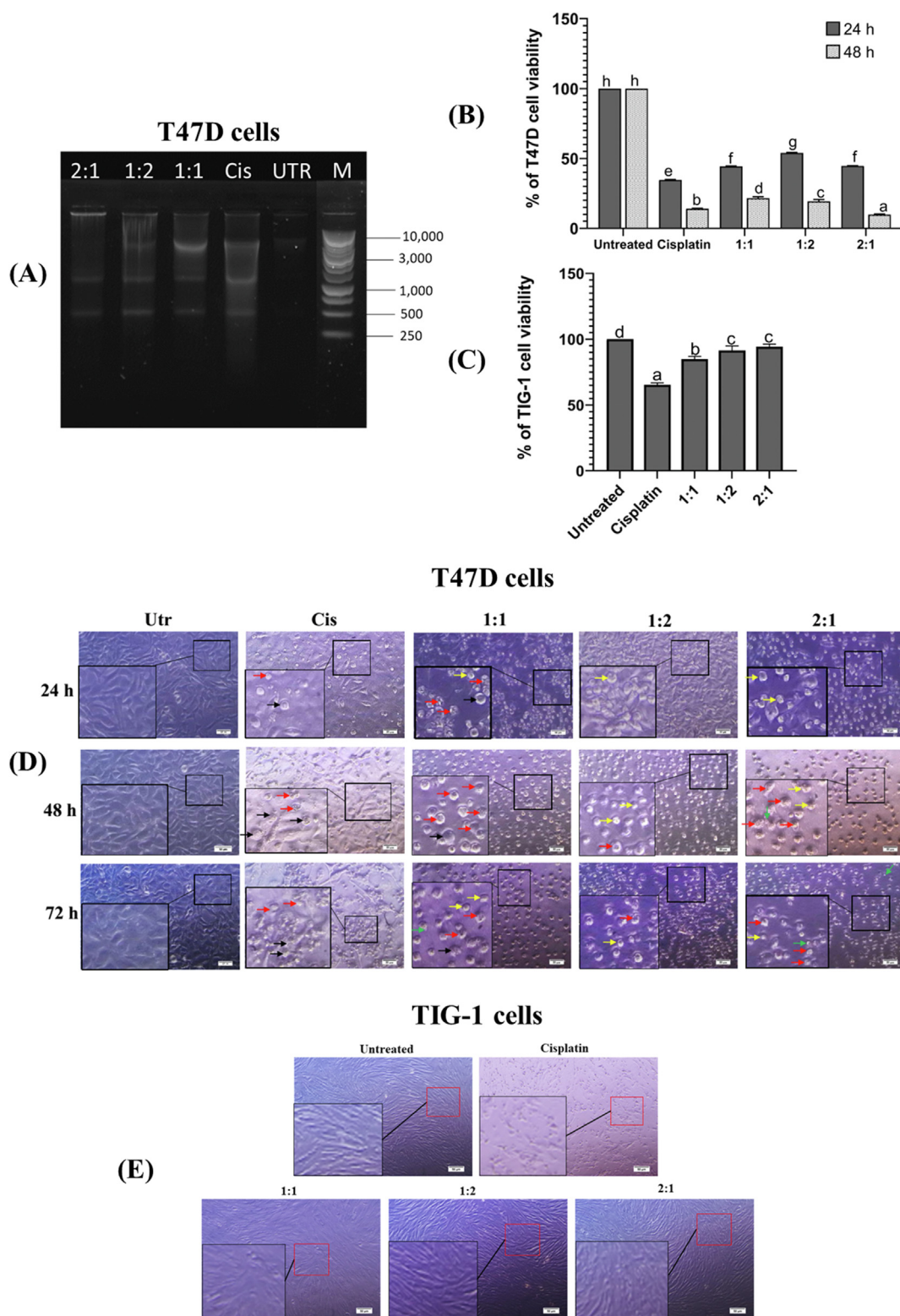
**Fig. 3.** The investigation of DNA fragmentation, cell viability and morphological changes in T47D cells after 24 and 48 h treatment with EL at different ratios (1:1, 1:2, and 2:1). (A) DNA fragmentation assay in T47D cell. Utr: untreated cells; Cis: cells treated with 1 μl/mL cisplatin. (B,C) Changes in cell viability of T47D and TIG-1 cells line. (E,D) Morphological assessment of T47D and TIG-1 using Olympus Inverted Microscopes Models IX71 (NY, USA) with 200× magnification. The apoptosis hallmark is indicated by nucleus condensation (yellow arrow), membrane blebbing (red arrow), apoptotic body (green arrow) and necrotic cell (black arrow). 1:1 = 1 × IC$_{50}$ value of *E. scaber* leaves and 1 × IC$_{50}$ value of *P. macrocarpa* leaves; 2:1 = 2 × IC$_{50}$ value of *E. scaber* leaves and 1 × IC$_{50}$ value of *P. macrocarpa* leaves; 1:2 = 1 × IC$_{50}$ value of *E. scaber* leaves and 2 × IC$_{50}$ value of *P. macrocarpa* leaves.
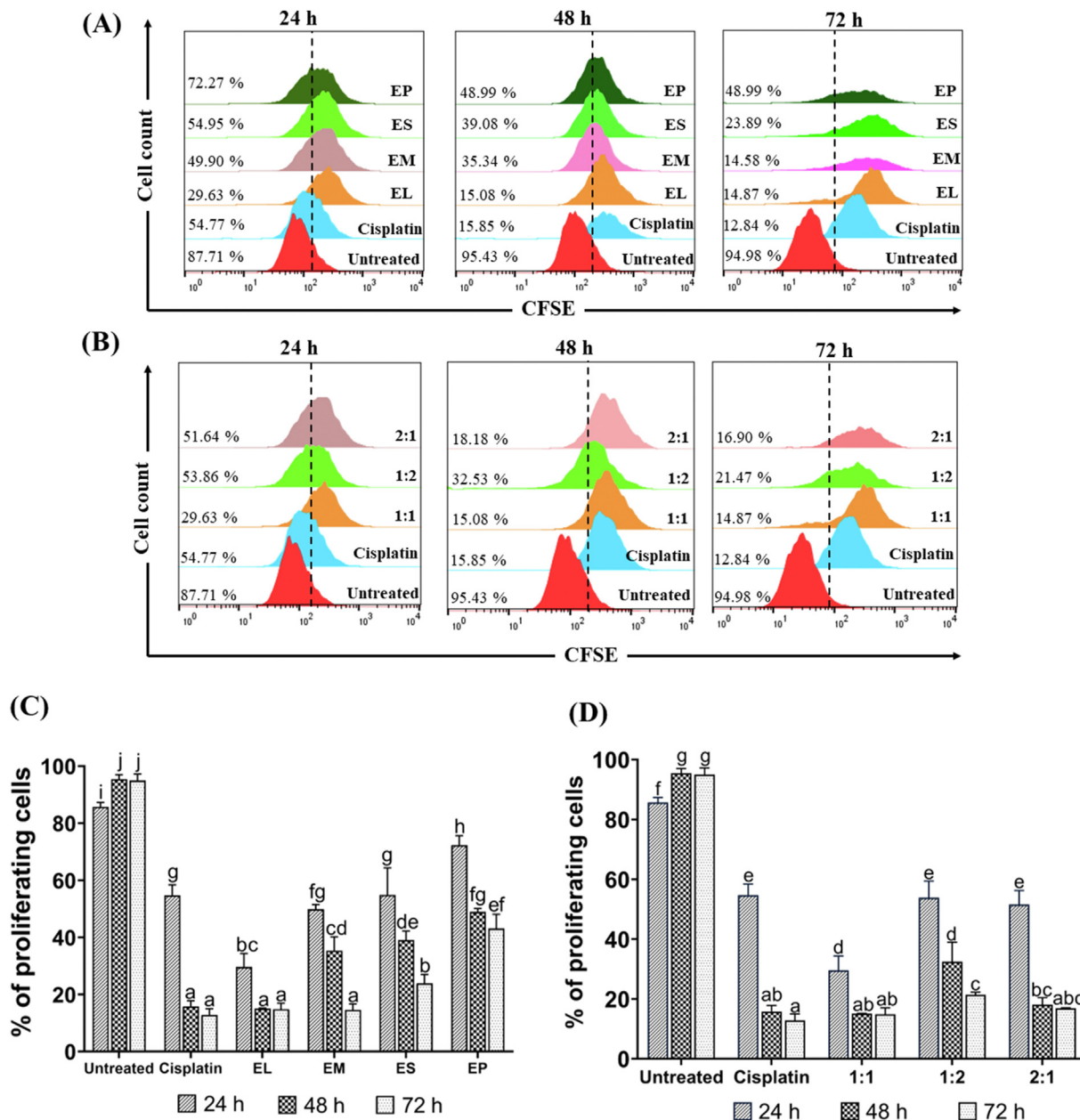
**Fig. 4.** Combination of *E. scaber* and *P. macrocarpa* inhibits proliferation of T47D cells. Fluorescence histogram of CFSE (carboxyfluorescein succinimidyl ester) labelled T47D cells after 24, 48 and 72 h treatment with (A) EL, EM, ES, and EP in ratio 1:1; and (B) three different ratio combinations of EL (1:1, 1:2, and 2:1). Untreated cells and cisplatin were set as negative and positive controls, respectively. The left population was separated by the dotted line representing T47D cells that were divided more than once. (C,D) The flow cytometry results were expressed as the percentage of proliferating T cells. Data were obtained from three independent experiments. Data are expressed as the mean of proliferating cells (%) $\pm$ SD in response to treatment. The different letters indicated statistical differences (p < 0.05). EL: *E. scaber* + *P. macrocarpa* leaves; EM: *E. scaber* + *P. macrocarpa* mesocarp; ES: *E. scaber* + *P. macrocarpa* seed; EP: *E. scaber* + *P. macrocarpa* pericarp; 1:1 = 1 $\times$ IC$_{50}$ value of *E. scaber* leaves and 1 $\times$ IC$_{50}$ value of *P. macrocarpa* leaves; 2:1 = 2 $\times$ IC$_{50}$ value of *E. scaber* leaves and 1 $\times$ IC$_{50}$ value of *P. macrocarpa* leaves; 1:2 = 1 $\times$ IC$_{50}$ value of *E. scaber* leaves and 2 $\times$ IC$_{50}$ value of *P. macrocarpa* leaves.

Gly390, His356, Leu327, Ley387, Met357, and Phe445. While sesamin bonds to ER-α through one hydrogen bond on Arg394 and eight van der Waals forces on Glu323, Gly442, His356, Ile326, Ile386, Lys449, Phe445, and Pro325. The identification of interacting amino acid residues revealed that both compounds had the same amino acid residues with tamoxifen, including Gly390, Lys449 and Phe445. Furthermore, Phe445 has appeared in all complexes except oleanolic acid-ERα. This molecular docking analysis supports our in vitro results, demonstrating that the EL combination greatly affected the relative number of ERα in T47D cells.

The molecular docking analysis also demonstrated that three compounds had the best binding affinity to bind with Nrf2, including oleanolic acid (10.6 kcal/mol), scutellarin (−10.1 kcal/mol) and sesamin (−9.9 kcal/mol). The binding affinity of these compounds was lower than AEM1 (−8.8 kcal/mol), as an Nrf2 inhibitor. Furthermore, these compounds had the same binding position as AEM1 (Fig. 7), which is indicated by the same amino acid residues of Nrf2. Oleanolic acid bound Gly367, Ile559, Val467, and Val606 through hydrogen bonds (Table 1). This compound has the highest binding affinity and bond to Nrf2 at a similar site as AEM1 than other compounds.
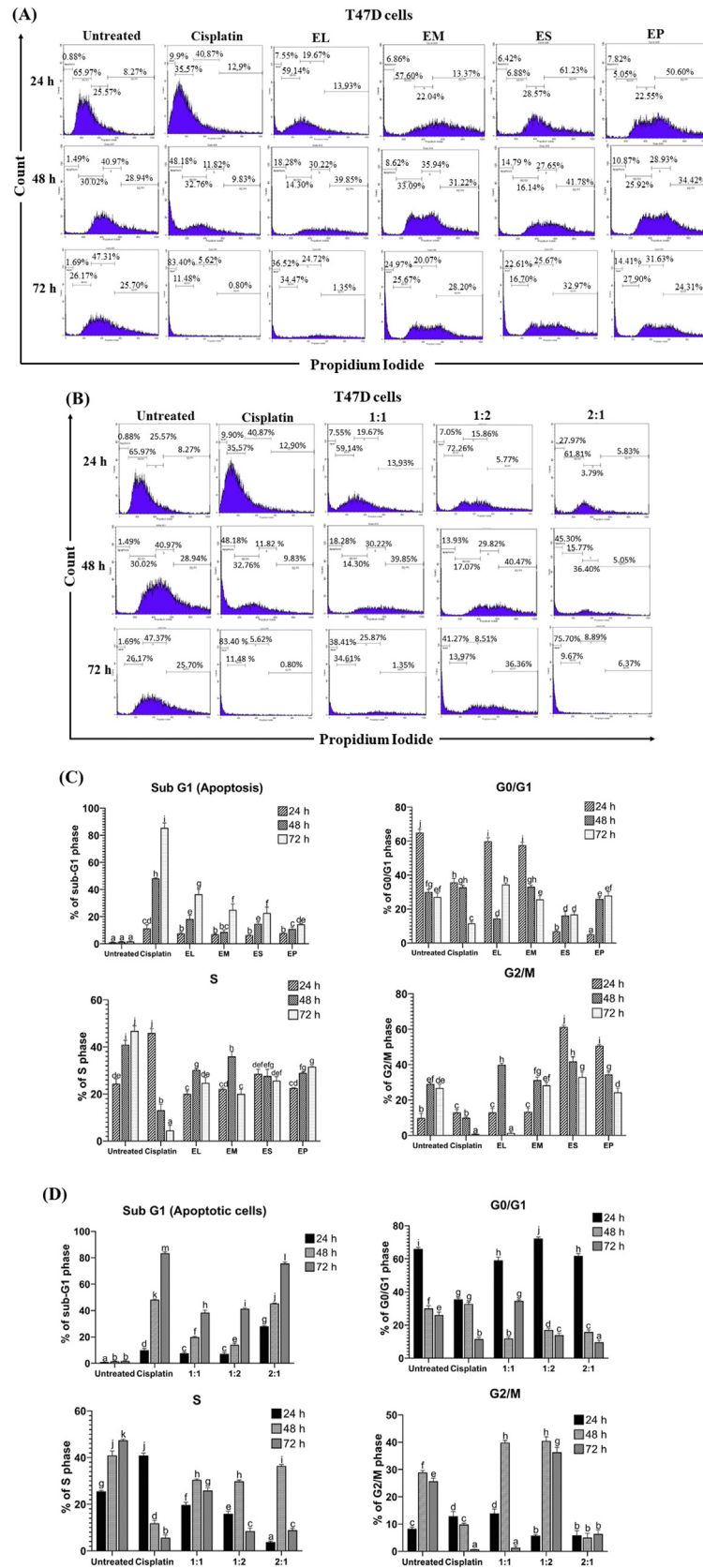
**Fig. 5.** The combination of *E. scaber* and *P. macrocarpa* leaves caused cell cycle arrest in T47D cells. Flow cytometry histogram demonstrates cell cycle distribution in T47D cells treated with (A) EL, EM, ES, and EP in ratio 1:1 and (B) three different ratios of EL (1:1, 1:2, and 2:1) for 24, 48 and 72 h. Untreated cells and cisplatin were used as negative and positive controls, respectively. (B, D) Representative graph was obtained from three independent experiments and expressed as the mean ± SD. The different letters indicated statistical differences (p < 0.05). EL: *E. scaber* + *P. macrocarpa* leaves; EM: *E. scaber* + *P. macrocarpa* mesocarp; ES: *E. scaber* + *P. macrocarpa* seed; EP: *E. scaber* + *P. macrocarpa* pericarp; 2:1 = 2 × IC$_{50}$ value of *E. scaber* leaves and 1 × IC$_{50}$ value of *P. macrocarpa* leaves; 1:2 = 1 × IC$_{50}$ value of *E. scaber* leaves and 2 × IC$_{50}$ value of *P. macrocarpa* leaves.
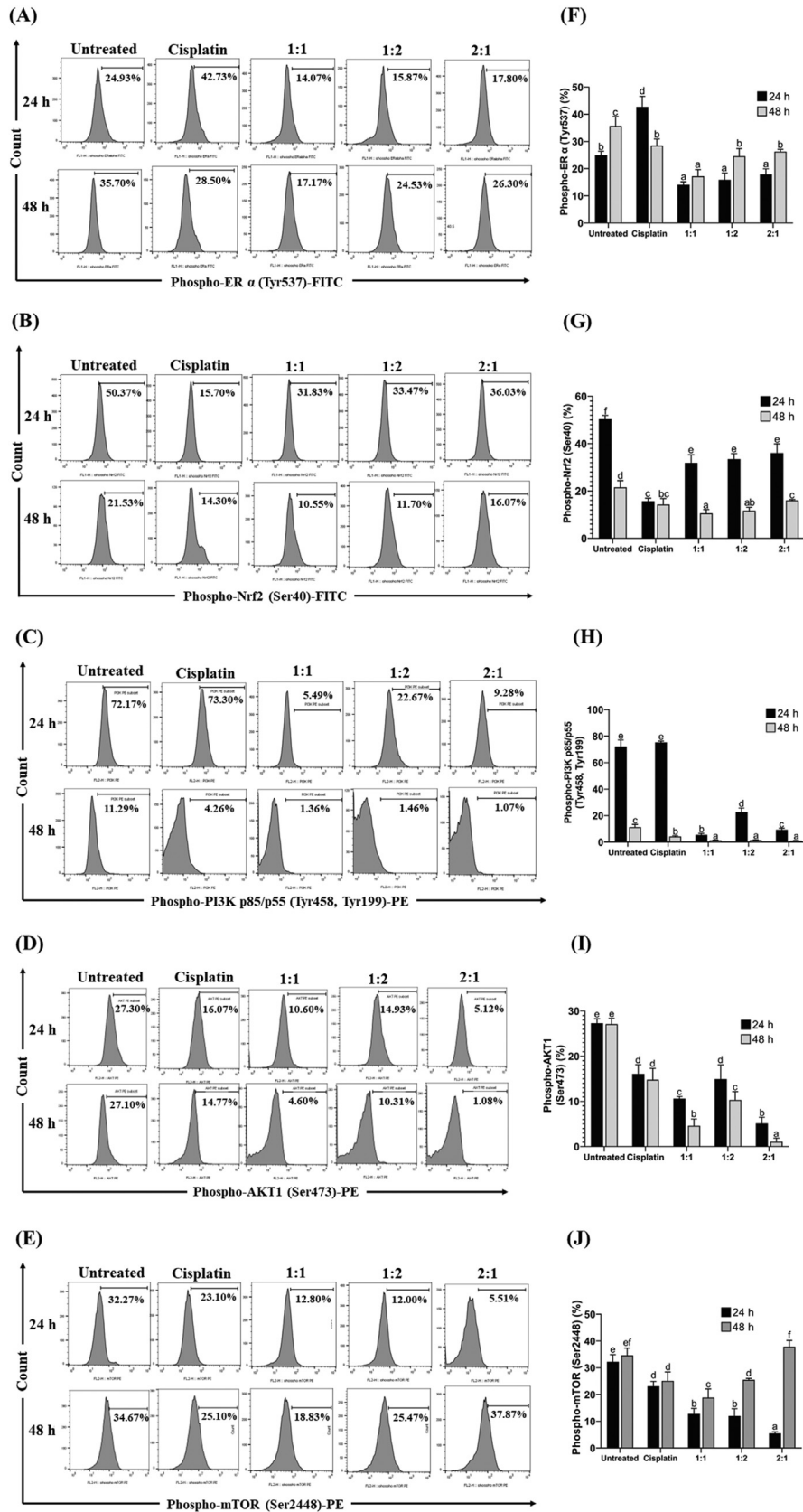
**Fig. 6.** The relative number of p-ER-α, p-Nrf2, p-PI3K, p-AKT and p-mTOR on T47D cells after being exposed to different ratios of EL (1:1, 1:2, and 2:1) for 24 and 48 h. Untreated cells and cisplatin were used as negative and positive controls, respectively. (A–E) Representative histogram of p-ER-α, p-Nrf2, p-PI3K, p-AKT and p-mTOR by flow cytometry analysis. (F–J) The graph was obtained from three independent experiments and expressed as the mean ± SD. The different letters indicated statistical differences (p < 0.05).
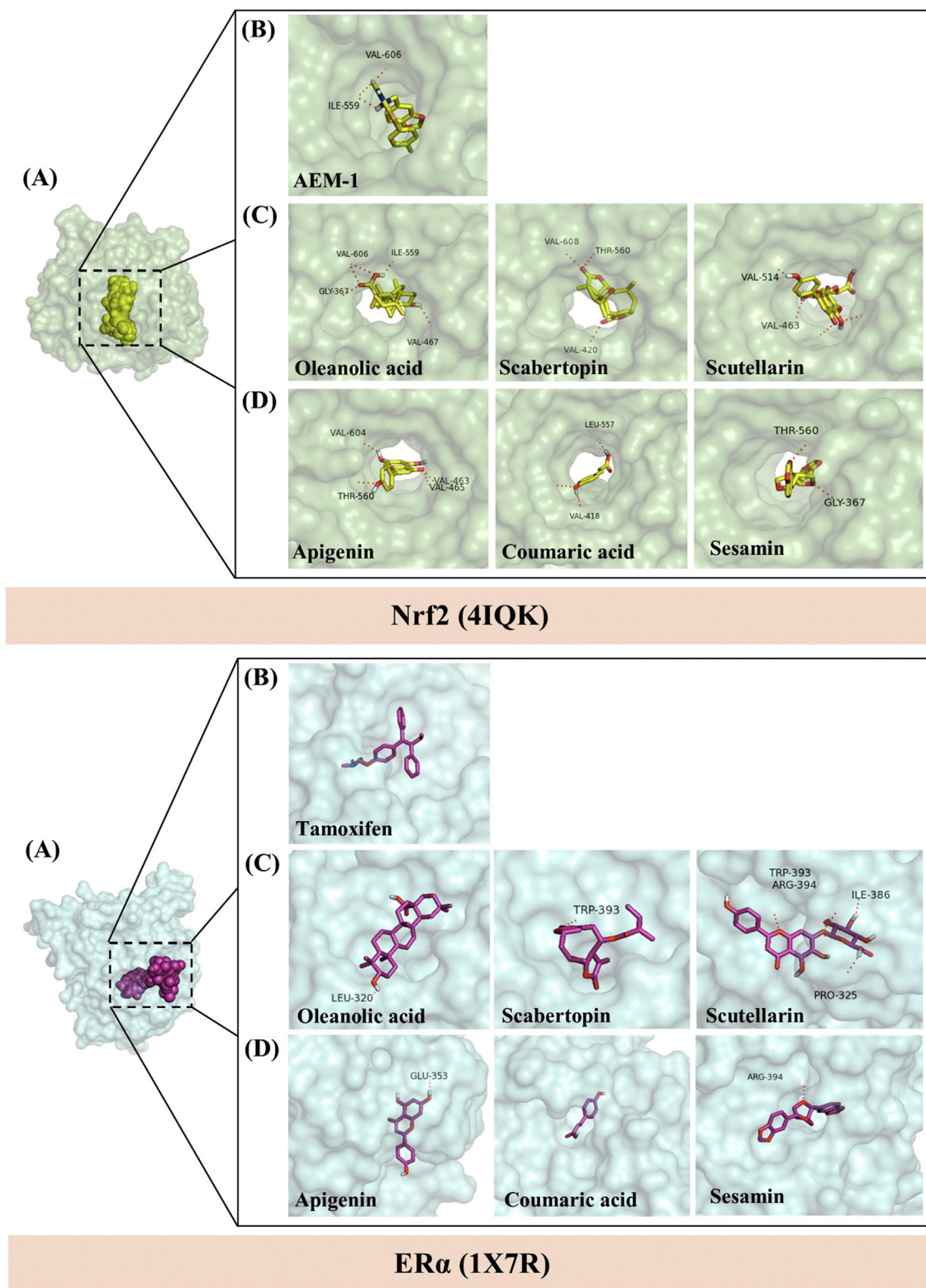
**Fig. 7.** Three-dimensional structure of ligand interacting with ER-α and Nrf2.

## 4. Discussion

Breast cancer is commonly known as aggressive cancer, which exhibits high mortality rates and poor prognosis. Even though chemotherapy is one of the effective therapy for breast cancer with high side effects, it should not be considered for long-term use. Thus, it is crucial to develop an alternative therapy that is more effective in killing cancer cells without producing severe side effects [23]. The research on the anticancer activity of *P. macrocarpa* leaves is limited. Many research focused on the

**Table 1**
The interaction of the selected compound of *E. scaber* and *P. macrocarpa* leaves with ERα and Nrf2

| Protein | Ligands | Binding Affinity (kcal/mol) | Hydrogen bonds | Van der Waals force |
|---|---|---|---|---|
| ERα | Tamoxifen | −6.7 | − | **Gly390**, Leu320, **Leu387**, Leu403, **Lys449**, **Phe445**, Pro324, Val446 |
| | Oleanolic acid | −6.4 | Leu320 | Asp321, Glu323, Trp393 |
| | Scabertopin | −6.4 | Trp393 | Glu323, Leu320, **Phe445** |
| | Scutellarin | −7.6 | Arg394, Ile386, Pro325, Trp393 | Glu353, Glu397, **Gly390**, His356, Leu327, Ley387, Met357, **Phe445** |
| | Apigenin | −7.6 | Glu353 | His356, Ile386, Leu327, Leu354, **Leu387**, Met357, **Phe445**, Pro325, Trp393 |
| | Coumaric acid | −5.7 | − | Arg394, Glu326, **Gly390**, His356, Ile386, Leu354, **Leu387**, Lys449, Met357, **Phe445** |
| | Sesamin | −8.5 | Arg394 | Glu323, Gly442, His356, Ile326, Ile386, **Lys449**, **Phe445**, Pro325 |
| Nrf2 | AEM1 | −8.8 | **Ile559**, **Val606** | **Ala466**, **Ala607**, **Gly417**, **Gly419**, **Gly511**, **Gly558**, **Gly605**, **Ile416**, **Leu365**, **Leu557**, **Val418**, **Val512**, **Val604**, **Val608** |
| | Oleanolic acid | −10.6 | Gly367, **Ile559**, Val467, **Val606** | **Ala466**, Ala510, **Ala607**, Cys368, Cys513, **Gly419**, Gly464, **Gly511**, **Gly558**, **Gly605**, **Leu557**, Thr560, **Val418**, Val463, **Val512** |
| | Scabertopin | −8.2 | Thr560, Val420, Val608 | **Ala466**, **Ala607**, Cys368, Gly367, Gly419, Ile559, **Val418**, Val465, **Val512** |
| | Scutellarin | −10.1 | Val463, Val514 | Ala510, Ala556, Arg415, Cys368, Gly364, Gly367, **Gly417**, **Gly419**, Gly462, Gly509, **Gly511**, **Gly558**, Gly603, **Ile416**, Ile559, **Leu365**, Leu515, **Leu557**, Thr560, **Val418**, Val465, **Val512**, **Val604** |
| | Apigenin | −8.7 | Thr560, Val463, Val465, Val604 | **Ala607**, Cys513, Gly367, **Gly417**, Gly464, **Gly558**, Gly603, **Gly605**, **Ile416**, Ile559, **Leu365**, **Leu557**, **Val418**, **Val512**, Val561, Val606 |
| | Coumaric acid | −6.1 | Leu557, Val418 | Ala556, Gly364, Gly367, **Gly417**, **Gly419**, Gly464, **Gly558**, Gly603, **Gly605**, **Ile416**, **Leu365**, Val463, Val465, **Val604** |
| | Sesamin | −9.9 | Gly367, Thr560 | **Ala607**, Cys368, Gly364, **Gly417**, **Gly419**, Gly509, **Gly558**, Gly603, **Gly605**, **Ile416**, Ile559, **Leu365**, **Leu557**, **Val418**, Val463, Val465, Val561, **Val604** |

whole fruit and seed to eliminate cancer cells [15]. Amir et al. [24] revealed that the methanol extract of *P. macrocarpa* leaves had been proven to inhibit the growth of MCF-7 cell lines with an IC$_{50}$ value of 15 μg/mL. When the concentration of the extract is high or low from the IC$_{50}$ value, the viability of the MCF-7 cell line is increased [24]. Our previous study investigated the single extract of *P. macrocarpa* leaves for their anticancer activity against T47D cells in-vitro [16]. A single extract of *E. scaber* also causes a decrease in the relative number of proinflammatory cytokines in mice after exposure to DMBA [25].

Our results showed that the EL group was the best combination to inhibit the growth of T47D cells. EL possessed the highest accumulation of apoptotic cells without producing high necrotic cells compared to cisplatin. According to Xu et al. [26], cisplatin could induce apoptosis and necrosis in cancer cells, which is indicated by the high necrosis markers of RIPK1 and RIPK3. EL decreased proliferating cells indicated an expansion of sub G1 and G0/G1 phase and a high S and G2/M phase reduction. Furthermore, EL at a ratio of 2:1 showed a notable decrease in the live cell by triggering late apoptosis after 72 h of incubation without producing more necrotic cells. After 48 and 72 h treatment with EL, the relative number of proliferating cells was not significantly different. Several possible reasons can be explained. First, maybe EL optimally decreased the proliferating cells only at 24 and 48 h. Second, perhaps the number of absorbed bioactive compounds by the cells was low after a long incubation. Therefore, EL loose toxicity after 48 h. Third, cancer cells have the ability to enhance the efflux of the extract and increase DNA repair capacity. Thus, after 72 h, EL induced a little cell death. However, in the next experiment, the observation after 72 h treatment (up to 72 h) should be done to confirm that EL works at time-dependent.

T47D is one of the human breast cancer cell lines with estrogen receptor alpha positive (ER+) [27]. The role of ERα is mainly contributed to the initiation and progression of the growth of breast cancer [28]. Several drugs were used in the therapy for ER-positive breast cancer, including fulvestrant, tamoxifen and letrozole [28,29]. This therapy inhibited ER signalling pathway that mediates estrogen stimulation in breast cancer cells [30]. Therefore, exploring selective ERα antagonists is essential to developing a new treatment for ER-positive breast cancer. This study found that the

EL ratio of 1:1 reduced the relative number of p-ERα, followed by a high reduction in proliferating cells. In line with molecular docking results, scutellarin, sesamin, and apigenin had the potential role become ERα antagonists. Sesamin, scutellarin and apigenin strongly bind with ERα with Glu353 and Arg394 as key amino acid residues in inhibiting ERα.

The Nrf2/Keap1 pathway is a master regulator of oxidative stress and xenobiotic detoxification [31]. However, recent studies showed that aberrant activation of Nrf2 in cancer causes metabolic reprogramming, leading to resistance in radiotherapy and chemotherapy [32]. Metabolic reprogramming by aberrant Nrf2 expression will provide energy and metabolites to support the proliferation and promote metastasis formation in breast cancer [33,34]. The sustained Nrf2 activation is caused by KEAP1 mutation, which is observed in adenocarcinoma and breast cancer [35]. However, the activation of Nrf2 in normal cells leads to chemopreventive effects by suppressing ROS-dependent DNA damage and carcinogenesis [31]. This study revealed that T47D cells constitutively expressed Nrf2 at a relatively high level and exhibited high sensitivity to cisplatin and EL. Based on molecular docking results, we hypothesize that oleanolic acid and scutellarin from *E. scaber* extract and sesamin from *P. macrocarpa* may stabilize the molecular interaction between KEAP1 and Nrf2 and then inhibit the translocation of Nrf2 to the nucleus. If the Nrf2 is inactive, the cell fails to prevent oxidative stress, leading to cell death. This hypothesis was supported by in vitro study that all ratios of EL significantly decreased Nrf2 levels.

The phosphatidylinositol-3-kinase (PI3K) pathway regulates cell cycle progression because this pathway is important for the DNA synthesis of the cells. The activated PI3K could catalyze the phosphorylation of AKT and then indirectly or directly activate its downstream protein, including NF-κB and mTOR [17]. AKT can activate mTOR through phosphorylation of TSC2 (tuberous sclerosis complex 2) protein. TSC2 is a component of the TSC protein complex that acts as a GTPase activating protein (GAP) for Rheb [36]. GAP is an inhibitor of GTPase protein by stimulating the conversion of active GTPase-GTP to GTPase-GDP. In the GDP form, GTPase becomes inactive and cannot bind to its target, thus inhibiting the cell signaling pathway [37]. However, the activation of AKT caused TSC2 to become inactive. Therefore, Rheb-GDP (inactive) becomes Rheb-GTP(Active) which then activates mTORC1. The activation of mTOR

leads to activate gene-related metabolism and cell growth [36]. In a recent study, GAP dysregulation promotes tumor growth and survival [37].

Our study demonstrated that untreated T47D cells exerted a high relative number of p-PI3K, p-AKT and p-mTOR, leading to high cell division. In line with Liu et al. [38], this pathway is highly activated in breast cancer, resulting in multidrug resistance. Activating PI3K/AKT requires synergistic transduction upstream and downstream to cause multidrug resistance. PI3K/AKT/mTOR causes dysregulation of micro-RNA and then mediates tumorigenesis [39]. Our previous in silico study revealed that corymboside could inhibit Bcl-2 expression, and sesamin stimulated the expression of caspase-3 and Bax protein [21]. The present study proved that EL notably declined the relative number of p-PI3K, p-AKT and p-mTOR with the optimal ratio of 2:1. The suppression of this pathway could promote apoptosis and cell cycle arrest and inhibit cell proliferation of T47D cells. The upregulation of PI3K is caused by the mutation or over-expression of upstream receptor tyrosine kinases (RTKs) and the loss of function of PTEN as PI3K regulator [40]. Recent studies have indicated crosstalk between PI3K and estrogen receptor (ER). During PI3Kα inhibition, ER could activate SGK1 protein levels, resulting in the high phosphorylation of KMT2D, suppressing its function and attenuating ER-dependent expression. The highly active SGK1 will inhibit ER activity [41].

Three bioactive compounds of *P. macrocarpa* leaves, including apigenin, coumaric acid and sesamin, were selected according to our previous study. Those compound has been predicted to have apoptosis activity [20]. Three selected compounds from *E. scaber* leaves extract (oleanolic acid, scabertopin, scutellarin) were also obtained from our previous study (in review). Based on molecular docking results, oleanolic acid and scutellarin from *E. scaber* leaves and sesamin from *P. macrocarpa* leaves can inhibit ERα and Nrf2, which are indicated by the lowest binding affinity and have the same binding position with drug control. The inhibition of the crosstalk effect between PI3K/AKT/mTOR, ERα and Nrf2 signaling pathway is necessary to develop a promising treatment for breast cancer. Our in silico study confirmed that the possible mechanism of reducing T47D cell growth by EL is by inhibiting both ER-α and Nrf2, resulting in the reduction in the crosstalk effect between Nrf2, ERα and PI3K/AKT/mTOR pathways. Therefore, this study proved that the bioactive of *E. scaber* and *P. macrocarpa* leaves inhibited breast cancer growth by triple inhibiting p-Nrf2, p-ERα and PI3K/AKT/mTOR signalling pathways.

## 5. Conclusion

The combination of *E. scaber* and *P. macrocarpa* leaves effectively suppressed the cell viability, induced apoptosis, inhibited the cell division and arrested the cell cycle of T47D cells by downregulating p-Nrf2, p-ERα and p-PI3K/AKT/mTOR signalling pathway. These findings suggest that EL at a ratio of 2:1 could be exploited to increase their therapeutic activity in vivo.

## Ethical approval

The study was approved by the Animal Care and Use Committee of Brawijaya University with approval number: 025-KEP-UB-2021.

## Source of funding

## Author contribution

Yuyun Ika Christina: Conceptualization, methodology, data collection, writing the manuscript, critical review.

Muhaimin Rifa'i: Data analysis, interpretation, writing the manuscript.

Nashi Widodo: Data visualization, critical review, writing the manuscript.

Muhammad Sasmito Djati: Supervision, critical review and editing, writing the manuscript.

## Declaration of Competing Interest

None.

## Acknowledgement

## References

[1] Laskar YB, Lourembam RM, Mazumder PB. In: Hassan BAR, editor. Herbal remedies for breast cancer prevention and treatment, medicinal plants. Use in prevention and treatment of diseases. London: IntechOpen Limited; 2020. https://doi.org/10.5772/intechopen.89669.

[2] Sung HS, Ferlay J, Siegel RL, Laversanne M, Soerjomataram I, Jemal A, et al. Global cancer statistics 2020: GLOBOCAN estimates of incidence and mortality worldwide for 36 cancers in 185 countries. Ca - Cancer J Clin 2021;71(3): 209–49. https://doi.org/10.3322/caac.21660.

[3] Kooti W, Servatyari K, Behzadifar M, Asadi-Samani M, Sadeghi F, Nouri B, et al. Effective medicinal plant in cancer treatment, Part 2: review study. J Evid Based Complementary Altern Med 2017;22(4):982–95. https://doi.org/10.1177/2156587217696927.

[4] Adjiri A. Identifying and targeting the cause of cancer is needed to cure cancer. Oncol Ther 2016;4(1):17–33. https://doi.org/10.1007/s40487-015-0015-6.

[5] Greenwell M, Rahman PKSM. Medicinal plants: their use in anticancer treatment. Int J Pharmaceut Sci Res 2015;6(10):4103–12. https://doi.org/10.13040/IJPSR.0975-8232.6(10).4103-12.

[6] Ochwang'i DO, Kimwele CN, Oduma JA, Gathumbi PK, Mbaria JM, Kiama SG. Medicinal plants used in treatment and management of cancer in Kakamega County, Kenya. J Ethnopharmacol 2014;151(3):1040–55. https://doi.org/10.1016/j.jep.2013.11.051.

[7] Beeran AA, Maliyakkal N, Rao CM, Udupa N. The enriched fraction of *Elephantopus scaber* triggers apoptosis and inhibits multi-drug resistance transporters in human epithelial cancer cells. Phcog Mag 2015;11(42):257–68. https://doi.org/10.4103/0973-1296.153077.

[8] Christina YI, Diana MR, Fuzianingsih EN, Nurhayati N, Ridwan FN, Widodo W, et al. Hormone-balancing and protective effect of combined extract of *Sauropus androgynus* and *Elephantopus scaber* against *E. coli*-induced renal and hepatic necrosis in pregnant mice. J Ayurveda Integr Med 2020;12(2):245–53. https://doi.org/10.1016/j.jaim.2020.09.001.

[9] Djati MS, Dwijayanti DR, Rifa'i M. Herbal supplement formula of *Elephantopus scaber* and *Sauropus androgynus* promotes IL-2 cytokine production of CD4+T cells in pregnant mice with typhoid fever. Open Life Sci 2016;11(1):211–9. https://doi.org/10.1515/biol-2016-0029.

[10] Djati MS, Rahma YA, Dwijayanti DR, Rifa'i M, Rahayu S. Synergistic effect of *Elephantopus scaber* L and *Sauropus androgynus* L merr extracts in modulating prolactin hormone and erythropoiesis in pregnant typhoid mice. Trop J Pharmaceut Res 2017;16(8):1789–95. https://doi.org/10.4314/tjpr.v16i8.6.

[11] Hiradeve SM, Rangari VD. *Elephantopus scaber* Linn: a review on its ethno-medical, phytochemical and pharmacological profile. J Appl Biomed 2014;12(2):49–61. https://doi.org/10.1016/j.jab.2014.01.008.

[12] Pitchai D, Roy A, Ignatius C. In vitro evaluation of anticancer potentials of lupeol isolated from *Elephantopus scaber* L. on MCF-7 cell line. "J Adv Pharm Technol Research" "(JAPTR)" 2014;5(4):179–84. https://doi.org/10.4103/2231-4040.143037.

[13] Jemal A, Siegel R, Ward E, Murray T, Xu J, Thun MJ. Cancer statistics. Ca - Cancer J Clin 2007;57(1):43–66. https://doi.org/10.3322/canjclin.57.1.43. 2007.

[14] Alara OR, Alara JA, Olalere OA. Review on *Phaleria macrocarpa* pharmacological and phytochemical properties. Drug Des 2016;5(3):1–5. https://doi.org/10.4172/2169-0138.1000134.

[15] Lay MM, Karsani SA, Banisalam B, Mohajer S, Malek SNA. Antioxidants, phytochemicals, and cytotoxicity studies on *Phaleria macrocarpa* (Scheff.) Boerl seeds. BioMed Res Int 2014:1–3. https://doi.org/10.1155/2014/410184.

[16] YI Christina, Rifa'i M, Widodo N, Djati MS. Comparative study of anti-proliferative activity in different plant parts of *Phaleria macrocarpa* and the

underlying mechanism of action. Sci World J 2022;2022:1−13. https://doi.org/10.1155/2022/3992660.

[17] Paplomata E, O'Regan R. The PI3K/AKT/mTOR pathway in breast cancer: targets, trials and biomarkers. Ther Adv Med Oncol 2014;6(4):154−66. https://doi.org/10.1177/1758834014530023.

[18] Fan J, Yin WJ, Lu JS, Wang L, Wu J, Wu FY, et al. ER alpha negative breast cancer cells restore response to endocrine therapy by combination treatment with both HDAC inhibitor and DNMT inhibitor. J Cancer Res Clin Oncol 2008;134(8):883−90. https://doi.org/10.1007/s00432-008-0354-x.

[19] Otieno JN, Hosea KM, Lyaruu HV, Mahunnah RL. Multi-plant or single-plant extracts, which is the most effective for local healing in Tanzania? Afr J Tradit, Complementary Altern Med 2008;5(2):165−72. https://doi.org/10.43142/ajtcam.v5i2.31269. 22.

[20] Djati MS, YI Christina, Rifa'i M. The combination of *Elephantopus scaber* and *Sauropus androgynus* promotes erythroid lineages and modulates follicle-stimulating hormone and luteinizing hormone levels in pregnant mice infected with *Escherichia coli*. Vet World 2021;14(5):1398−404. https://doi.org/10.14202/vetworld.2021.1398-1404.

[21] YI Christina, Nafisah W, Atho'illah MF, Rifa'i M, Widodo N, Djati MS. Anti-breast cancer potential activity of Phaleria macrocarpa (Scheff.) Boerl. leaf extract through in silico studies. J Pharm Pharmacogn Res 2021;9(6):824−45. 2021.

[22] Atho'illah MF, Safitri YD, Nur'aini FD, Widyarti S, Tsuboi H, Rifa'i M. Elicited soybean extract attenuates proinflammatory cytokines expression by modulating TLR3/TLR4 activation in high-fat, high-fructose diet mice. J Ayurveda Integr Med 2021;12(1):43−51. https://doi.org/10.1016/j.jaim.2021.01.003.

[23] Zhu HY, Huang HY, Wu YL. Anticancer and apoptotic activities of oleanolic acid are mediated through cell cycle arrest and disruption of mitochondrial membrane potential in HepG2 human hepatocellular carcinoma cells. Mol Med Rep 2015;12(4):5012−8. https://doi.org/10.3892/mmr.2015.4033.

[24] Amir H, Murcitro BG, Ahmad AS, Kassim MNI. The potential use of phaleria macrocarpa leaves extract as an alternative drug for breast cancer among women living in poverty. Asian J Poverty Stud 2017;3(2):138−45. https://doi.org/10.33369/ajps.v3i2.2691.

[25] Amalia R. Pengaruh Ekstrak *Elephantopus scaber* terhadap sistem imunitas pada Mus Musculus yang diinduksi senyawa karsinogen dmba dan hormon Esterogen (effect of *Elephantopus scaber* extract on the immune System in Musculus induced by DMBA carcinogen compounds and estrogen hormones [Magister thesis]. Malang, Indonesia: University of Brawijaya; 2018.

[26] Xu Y, Lin Z, Zhao N, Zhou L, Liu F, Cichacz Z, et al. Receptor interactive protein kinase 3 promotes Cisplatin-triggered necrosis in apoptosis-resistant esophageal squamous cell carcinoma cells. PLoS One 2014;9(6):e100127. https://doi.org/10.1371/journal.pone.0100127.

[27] Zhu Y, Wang A, Liu MC, Zwart A, Lee RY, Gallagher A, et al. Estrogen receptor alpha positive breast tumors and breast cancer cell lines share similarities in their transcriptome data structures. Int J Oncol 2006;29(6):1581−9.

[28] Sharma D, Kumar S, Narasimhan B. Estrogen alpha receptor antagonists for the treatment of breast cancer: a review. Chem Cent J 2018;12(1):1−32. https://doi.org/10.1186/s13065-018-0472-8.

[29] Nunnery SE, Mayer IA. Targeting the PI3K/AKT/mTOR pathway in hormone-positive breast cancer. Drugs 2020;80(16):1685−97. https://doi.org/10.1007/s40265-020-01394-w.

[30] Fan J, Yin WJ, Lu JS, Wang L, Wu J, Wu FY, et al. ER alpha negative breast cancer cells restore response to endocrine therapy by combination treatment with both HDAC inhibitor and DNMT inhibitor. J Cancer Res Clin Oncol 2008;134(8):883−90. https://doi.org/10.1007/s00432-008-0354-x.

[31] Aliyev AT, Panieri E, Stepanić V, Gurer-Orhan H, Saso L. Involvement of NRF2 in breast cancer and possible therapeutical role of polyphenols and melatonin. Molecules 2021;26(7):1−18. https://doi.org/10.3390/molecules26071853.

[32] Wang YY, Chen J, Liu XM, Zhao R, Zhe H. Nrf2-mediated metabolic reprogramming in cancer. Oxid Med Cell Longev 2018;2018:1−7. https://doi.org/10.11552/F20182F9304091.

[33] Catanzaro E, Calcabrini C, Turrini E, Sestili P, Fimognari C. Nrf2: a potential therapeutic target for naturally occurring anticancer drugs? Expert Opin Ther Targets 2017;21(8):781−93. https://doi.org/10.1080/14728222.2017.1351549.

[34] Woo Y, Oh J, Kim JS. Suppression of Nrf2 activity by chestnut leaf extract increases chemosensitivity of breast cancer stem cells to paclitaxel. Nutrients 2017;9(7):1−15. https://doi.org/10.3390/nu9070760.

[35] Panieri E, Saso L. Potential applications of NRF2 inhibitors in cancer therapy. Oxid Med Cell Longev 2019;2019:1−34. https://doi.org/10.1155/2019/8592348.

[36] Miricescu D, Totan A, Stanescu-Spinu II, Badoiu SC, Stefani C, Greabu M. PI3K/AKT/mTOR signaling pathway in breast cancer: from molecular landscape to clinical aspects. Int J Mol Sci 2020;22(1):173. https://doi.org/10.3390/ijms22010173.

[37] Ji V, Kishore C. The emerging roles of srGAPs in cancer. Mol Biol Rep 2022;49:755−9. https://doi.org/10.1007/s11033-021-06872-2.

[38] Liu R, Chen Y, Liu G, Li C, Song Y, Cao Z, et al. PI3K/AKT pathway as a key link modulates the multidrug resistance of cancers. Cell Death Dis 2020;11(797):1−12. https://doi.org/10.1038/s41419-020-02998-6.

[39] Millis SZ, Jardim DL, Albacker L, Ross JS, Miller VA, Ali SM, et al. Phosphatidylinositol 3-kinase pathway genomic alterations in 60,991 diverse solid tumors informs targeted therapy opportunities. Cancer 2019;125(7):1185−99. https://doi.org/10.1002/cncr.31921.

[40] Vasan N, Toska E, Scaltriti M. Overview of the relevance of PI3K pathway in HR-positive breast cancer. Ann Oncol 2019;30(Suppl 10):x3−11. https://doi.org/10.1093/annonc/mdz281.

[41] Toska E, Castel P, Chhangawala S, Arruabarrena-Aristorena A, Chan C, Hristidis VC, et al. PI3K inhibition activates SGK1 via a feedback loop to promote chromatin-based regulation of ER-dependent gene expression. Cell Rep 2019;27(1):294. https://doi.org/10.1016/j.celrep.2019.02.111.